JOURNAL OF OPTOELECTRONICS AND ADVANCED MATERIALS, Vol. 12, No. 6, June 2010, p. 1273 - 1278

Sintering temperature effect and luminescent properties of Dy^{3+}:YAG nanophosphor

G. SEETA RAMA RAJU[a], HONG CHAE JUNG[a], JIN YOUNG PARK[a], JONG WON CHUNG[a], BYUNG KEE MOON[a*], JUNG HYUN JEONG[a], SE-MO SON[b], JUNG HWAN KIM[c]
[a]*Department of Physics, Pukyong National University, Busan 608-737, Republic of Korea*
[b]*Division of Image science and Information Engineering, Pukyong National University, Busan, 608739,Republic of Korea*
[c]*Department of Physics, Dong Eui University, Busan 614-714,Republic Korea*

A series of Dy^{3+} ions activated YAG nanophosphors have been prepared by means of solvothermal process and sintered at various temperatures. The crystalline structure and morphology of the samples were investigated by X-ray diffraction and scanning electron microscopy measurements. The synthesis, structural and luminescent properties along with chromaticity coordinates of the nanophosphor samples with the compositions xDy: $Y_{(3-x)}Al_5O_{12}$ (x=0.5 to 5 mol%) are featured in this paper. Furthermore, the yellow to blue intensity ratio of Dy^{3+} ions activated YAG system nanophosphors varies from 0.71 to 0.54. Such luminescent powders are expected to find potential applications such as optical display systems and lamps.

(Received November 23, 2009; accepted June 16, 2010)

Keywords: Optical materials, Thermogravimetric analysis (TGA), X-ray diffraction, Luminescence

1. Introduction

The research on the trivalent rare earth (RE^{3+}) ions activated inorganic luminescent materials (also called phosphors) continues to be an active research area, which may be attributed to the remarkable physical and chemical properties of these complexes and their applications in optoelectronic devices, temperature sensors, solid-state lighting (SSL) and luminescent probes or labels in biological systems and so on [1-5]. In recent years, interest in the RE^{3+} ions doped nanocrystalline host has increased due to their unique optical behavior and their attractive applications in the field of nanobiotechnology [6]. It is well known that yttrium aluminum garnet ($Y_3Al_5O_{12}$ or YAG) is one of the widely studied phosphor host materials with interesting optical and mechanical properties [7-9]. Initially in the early 1960s, single crystals of YAG have drawn attention for fluorescence and solid-state laser applications [10, 11]. In view of the expensiveness and difficulties involved in single crystal growth, the focus has now been shifted to polycrystalline YAG with ceramic processing techniques having advantages in preparation time, cost, and scale of production [12, 13]. YAG has cubic crystal structure with isotropic thermal expansion and absence of birefringence effects, which are favorable for the aforementioned properties [14]. Small amounts of different RE^{3+} activators are substituted into the dodecahedral site of YAG lattice to induce interesting luminescence characteristics. Furthermore Dy^{3+} ions can show strong luminescence in a variety of lattices and exhibit both blue ($^4F_{9/2}\rightarrow{}^6H_{15/2}$) and yellow ($^4F_{9/2}\rightarrow{}^6H_{13/2}$) emissions, which are necessary for the development of white light emission and are very useful in high resolution optical display systems, temperature sensors and lamps [15, 16].

Generally, YAG phosphors are prepared by traditional solid-state reaction method using yttrium oxide (Y_2O_3) and aluminum oxide (Al_2O_3) compounds. Due to insufficient mixing and low reactivity of raw materials, several intermediate phases such as $Y_4Al_2O_9$ (YAM) and $YAlO_3$ (YAP) easily coexist in the product. Repeated mechanical mixing and long heating durations are essential to eliminate these intermediate phases [17]. However, in recent years, several wet chemical techniques such as co-precipitation method, sol-ge1, combustion, hydrothermal synthesis and spray-pyrolysis synthesis were used to prepare the single phase phosphor [17-22]. These wet chemical processing methods offer an intimate mixing of starting materials and hence have shorter diffusion distances between reactants, requiring relatively low temperatures for final formation of products with excellent chemical homogeneity [23]. However, to achieve high crystallinity and transform the powder into a dense ceramic, sintering at elevated temperatures becomes mandatory. In this regard, the solid-state method still stands a practical option and the best emission efficiencies are often recorded by powders obtained from this method.

In this context, we have synthesized the Dy^{3+} activated YAG phosphor by means of solvothemal process with single phase at various sintering temperatures. To the best of our knowledge, a very few reports with fewer luminescent properties have been found on Dy^{3+}:YAG phosphors[24,25], but no reports have been found on Dy^{3+}:YAG nanophosphors by means of solvothermal process. In this paper, the first time we report on the synthesis, structural and luminescent properties of Dy^{3+}: YAG nanophosphors.

2. Experimental

A series of Dy^{3+} activated YAG nanophosphors were prepared by means of solvothermal process with the composition xDy^{3+}: $Y_{(3-x)}Al_5O_{12}$ (x=0.5 to 5 mol%). The stoichiometric amounts of high purity grade yttrium nitrate hexahydrate ($Y(NO_3)_3{\cdot}6H_2O$), dysprosium nitrate pentahydrate ($Dy(NO_3)_3{\cdot}5H_2O$), and aluminum isopropoxide {$[(CH_3)_2CHO]_3Al$} were dissolved in 40 ml of 2-propanol. All reagents were used without any further purification and stirred vigorously by using magnetic stirrer until the homogeneous solution was formed and transferred into a stainless steel autoclave with a Teflon liner (80ml capacity and 50 % filling). It was then heated to 230 ºC at a rate of 2ºC/min and maintained for 5h with magnetic stirring (at 180 rpm) to make stable networks of Y-O-Al and Dy-O-Al. After cooling gradually down to room temperature, the precipitate was separated by a centrifugal separator with 3000 rpm for 3 min and then dried at 50 ºC for a day in ambient atmosphere. The dried powder was sintered at different temperatures for 5h.

Characterization

Thermogravimetric/differential thermal analysis (TG/DTA) of the dried powder precursors were carried out with a *Material Analysis and Characterization TG-DTA 2000*. This experiment was carried out at a heating rate of 5 ºC/min and the samples were heated from room temperature to 1000 ºC. X-ray diffraction (XRD) patterns of sintered powders were recorded on *X' PERT PRO* X-ray diffractometer with CuK_α=1.5406Å. The morphology and the atomic wt% of the sintered particles were examined by means of scanning electron microscopy (SEM) along with EDX, model *HITACHI S-4200 FESEM*. Osmium coating was sprayed on the sample surfaces by using *Hitachi* fine coat ion sputter *E-1010* unit to avoid possible charging of specimens before SEM observation was made on each time. The room temperature photoluminescent spectra were recorded on a *PTI* (Photon Technology International) fluorimeter with a Xe-arc lamp of power 60W.

3. Results and discussion

Fig. 1 illustrates the TG/DTA curves of the YAG powder precursor. The TG curve of YAG shows three distinct weight loss steps up to 180 ºC, 470 ºC and 650ºC respectively; no further weight loss was registered up to 1000 ºC. The weight loss is related to the decomposition of organic matrix. The DTA curve consists of four exothermic peaks with maxima at 278 ºC, 384 ºC, 525 ºC and 930 ºC. The first three exothermic peaks indicating that the thermal events can be associated with the burnout of organic species involved in the precursor powders of the residual nitrates. The fourth exothermic peak is due to crystallization of YAG powder from the amorphous component. The crystallization temperature is well in agreement with the XRD analysis.

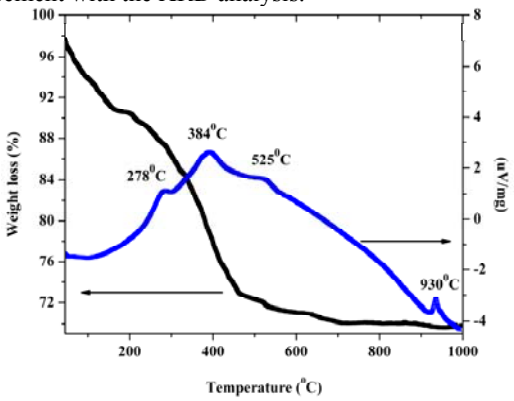

Fig 1. TG/DTA curves of YAG powder precursor.

Fig. 2 compares the XRD patterns of Dy^{3+} :YAG nanophosphor at various sintering temperatures and which confirm their cubic nature. The phosphor was found to be amorphous until the precipitate powders was sintering at 800 ºC and crystallized as pure YAG at 900 ºC without the formation of any intermediate phase, indicating that the powders prepared by solvothermal process is pure in both chemistry and crystalline phase. The diffraction peaks intensity and the crystallite size increases significantly with increasing the sintering

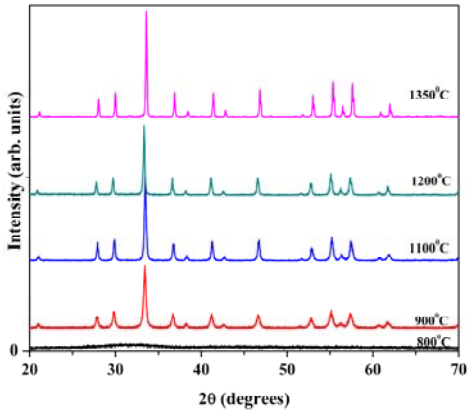

Fig 2. XRD patterns of Dy^{3+}:YAG nanophosphors at different sintering temperatures.

temperatures. At all sintering temperatures (900 ºC - 1350 ºC), the diffraction peaks are in well agreement with the standard JCPDS card [PDF (82-0575)] with space group Ia3*d*. In general, the crystallite size can be estimated by using the Scherrer's equation, $D_{hkl}=k\lambda/\beta\cos\theta$, where D is the average grain size, k=0.9 is shape factor, λ is the X-ray wavelength (1.5406Å), β is the full width at half maximum (FWHM) and θ is the diffraction angle of an observed peak, respectively. The strongest diffraction peaks are used to calculate the crystallite size of Dy^{3+}: YAG nanophosphor, sintered at 900 ºC, 1000 ºC, 1200 ºC ,

1350 ºC, which yield average values of about 35 nm, 44 nm, 56 nm and 78 nm respectively. The reason for the crystalline size increases is that the high energy supply from the high synthesis temperature improves nucleation and crystallization growth [26].

Fig. 3 shows the effect of sintering temperature, crystallite size, and emission intensity of the 1 mol% Dy^{3+}: YAG nanophosphor. The crystallite size and emission intensity increases with increasing the sintering temeperature as shown in Fig. 3(a). Fig. 3(b) also clears that the emission intensity increases gradually with increasing crystallite size. For this reason, remaining all measurements was carried out at higher temperature of 1350 ºC.

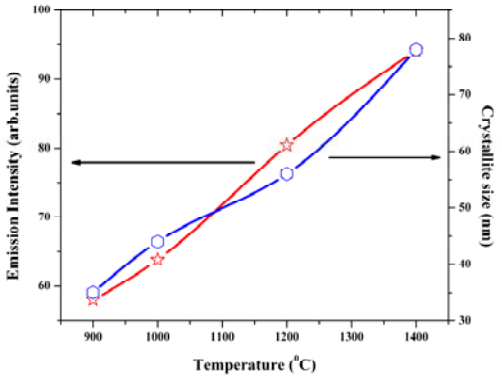

Fig 3(a). Relationship between sintering temperature-crystallite size and emission intensity

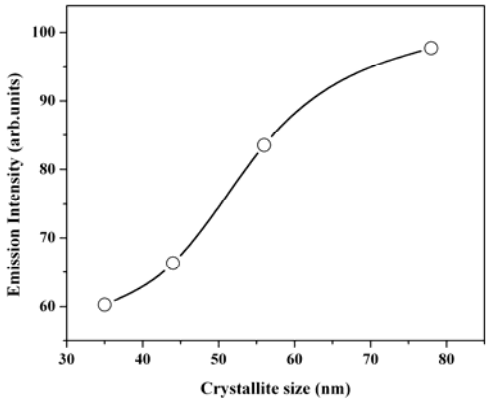

Fig 3(b) Relationship between crystallite size and emission intensity of Dy^{3+}:YAG nanophosphors

Fig. 4 shows the SEM image of Dy^{3+}: YAG nanophosphor and from which spherical shaped particles are noticed, those might be due to the occurrence of agglomerations amongst the YAG particles during the period of sample sintering at 1350°c for 5h. It is well known that spherical-shaped

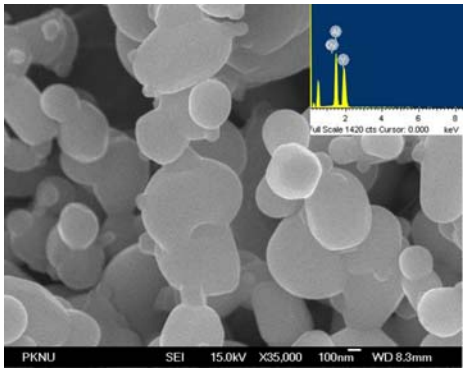

Fig. 4. SEM image of Dy^{3+}:YAG nanophosphor at 1350ºC sintering temperature.inset figure shows the EDX spectrum.

particles (≤ 2 μm) are of greater importance because of their high packing density, lower scattering of light and brighter luminescence performance. The energy dispersive X-ray (EDX) analysis was carried out to identify the compositions of phosphor as shown inset of the Fig. 4.

Fig. 5 presents the photoluminescence excitation (PLE) spectra (within the range of 200nm -500nm) of Dy^{3+}: YAG nanophosphors sintered at1350 ºC. The excitation spectra of Dy^{3+}: YAG nanophosphors were measured with the emission wavelength fixed at 482nm corresponding to the electronic transition ($^4F_{9/2}\rightarrow{}^6H_{15/2}$) and at all concentrations, the spectra show similar features except intensity. The excitation spectra consist of sharp lines due to the f-f transitions of Dy^{3+} ions, which are assigned to the electronic transitions ($^6H_{15/2}\rightarrow{}^6P_{3/2}$) at 326nm, ($^6H_{15/2}\rightarrow{}^6P_{7/2}$) at 352nm, ($^6H_{15/2}\rightarrow{}^6P_{5/2}$) at 366nm, ($^6H_{15/2}\rightarrow{}^4K_{17/2}$) at 379 nm, ($^6H_{15/2}\rightarrow{}^4I_{13/2}$) at 387nm, ($^6H_{15/2}\rightarrow{}^4F_{7/2}$) at 393nm, ($^6H_{15/2}\rightarrow{}^4G_{11/2}$) at 427nm and ($^6H_{15/2}\rightarrow{}^4I_{15/2}$) at 448 nm. In the same way, very weak Dy^{3+}-O^{2-} charge transfer state (CTS) bands was observed in the short wavelength range (285 nm -305 nm) and host absorption band (HAB) was not observed. This phenomenon also confirms that the Dy^{3+} interactions

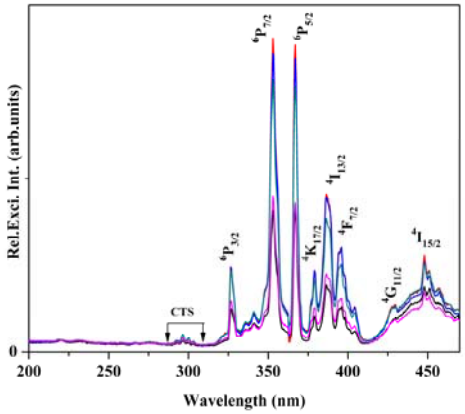

Fig 5. The PLE spectra of Dy^{3+}: YAG nanophosphors at 1350ºC sintering temperature

with host lattice are weak, and no energy transfer between Dy^{3+} and the host. The assignment of all the transitions of excitation and emission spectra are based on the earlier results of W.T Carnall et al. [27].

Fig.6 shows the photoluminescence (PL) spectra of Dy^{3+}: YAG nanophosphors sintered at 1350 °C, which were excited at 352 nm. The PL spectra shows the two main groups of lines in the blue region (460nm - 500nm) and yellow region (555nm - 610nm) and also some weak lines observed in red region. These blue, yellow, and red emissions

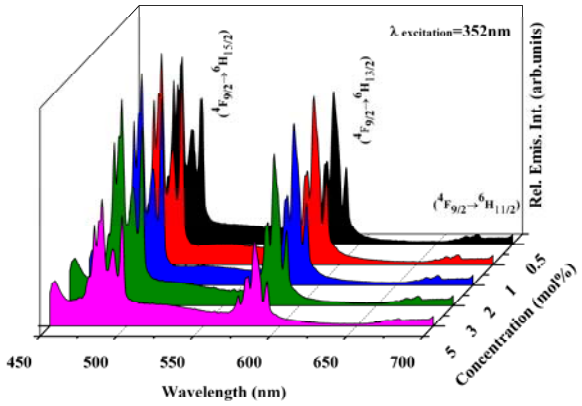

Fig 6. The PL spectra of Dy^{3+}:YAG nanophosphors at 1350°C sintering temperature

are assigned to the electronic transitions ($^4F_{9/2}\rightarrow{}^6H_{15/2}$), ($^4F_{9/2}\rightarrow{}^6H_{13/2}$) and ($^4F_{9/2}\rightarrow{}^6H_{11/2}$) respectively. The crystal field splitting components of Dy^{3+} can be observed and is well correlated with the Kramer's doublets (2J+1)/2, where J is the total angular momentum of the electrons [28,29]. It indicates that Dy^{3+} ions are well substituted into Y^{3+} sites. The integrated intensity of blue emission is greater than that of the yellow emission, this can be explained according to the following reason: It is well known that The blue ($^4F_{9/2}\rightarrow{}^6H_{15/2}$) emission corresponding to the magnetic dipole transition, which is insensitive to the crystal field symmetry around the Dy^{3+} ion and the yellow ($^4F_{9/2}\rightarrow{}^6H_{13/2}$) emission belongs to the hypersensitive (forced electric dipole) transition with the selection rule, $\Delta J=2$, which is strongly influenced by the outside surrounding environment. When Dy^{3+} is located at a low symmetry local site (without inversion symmetry), the yellow emission is often dominant in the emission spectrum and when Dy^{3+} is at a high symmetry local site (with inversion symmetry center), the blue emission is stronger than the yellow emission and is dominant in the emission spectrum [30]. The latter case occurs for Dy^{3+} doped YAG nanophosphors, this can also be explained according to the crystal structure of $Y_3Al_5O_{12}$. The cubic unit cell of a general garnet compound $C_3A_2D_3O_{12}$ contains eight formula units, where C, A, D are metal ions occupying different symmetry sites are shown in fig.7. It has a bcc structure (space group Ia3*d*) with 160 atoms in the cubic conventional cell. The Y ions (*C* atoms) occupy the 24(*c*) sites and each is dodecahedrally coordinated to eight O with D_2 point symmetry (with inversion center). There are two different sites for Al, Al_{oct} (*A* atoms) occupy the 16(*a*) site with octahedral point symmetry (C_{3i}) and Al_{tet} (*D* atoms) occupy the 24(*d*) sites with tetrahedral point symmetry (S_4) [31]. These structural units may show the different behavior to internal stresses, the dodecahedral unit being the less rigid one [32].

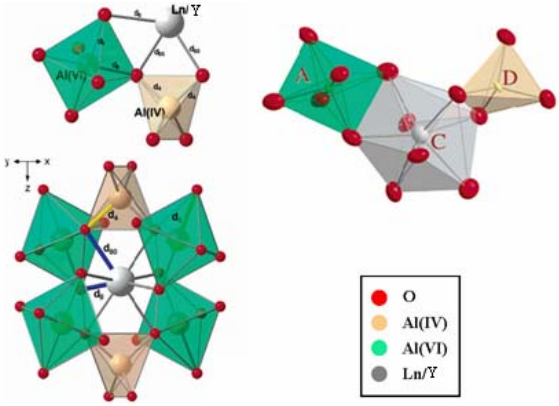

Fig 7. Magnified crystallographic unit cell of $Y_3Al_5O_{12}$ garnet system.

Considering the ionic radii, r (Dy^{3+}) =0.912Å (for octahedral site) and 1.027Å (for dodecahedron site), r (Y^{3+}) =1.019Å for dodecahedral site and r (Al^{3+}) = 0.39Å (for tetrahedral site) and 0.535Å(for octahedral site). It is easier for dodecahedral site of Dy^{3+} ions to replace the dodecahedral site of Y^{3+} ions than the other octahedral and tetrahedral sites of Al^{3+} ions in the YAG host lattice. The spectral property of the Dy^{3+} confirms that the Dy^{3+} ions occupy the dodecahedral Y^{3+} sites in the $Y_3Al_5O_{12}$ host lattice. When the concentration of Dy^{3+} increases from 0.5 to 1mol%, the emission intensity increases, and exceeds the concentration more than 1 mol%, the emission intensity decreases due to concentration quenching. The concentration quenching might be elucidated by two factors, (i) the excitation migration due to resonance between the activators is enhanced when the doping concentration is increased, and thus the excitation energy reaches quenching centers, and (ii) the activators are paired or coagulated and are changed to quenching center. Furthermore, the yellow to blue (Y/B) ratio also depends upon the concentration, and when the concentration increases from 0.5 to 1 mol%, the Y/B ratio also increases from 0.6 to 0.71 and when the concentration increases above 1 mol% the Y/B ratio decreases from 0.71 at 1 mo% to 0.65 at 2 mol%, 0.56 at 3 mol% and 0.54 at 5 mol%. This can be understood if one considers that the doping concentration of the Dy^{3+} ions in the host matrices may changes the degree of polarization of neighboring O^{2-} ions [30].

Fig. 8 shows the decay of the luminescence of the $^4F_{9/2}$ level of Dy^{3+}: YAG nanophosphors. The decay of Dy^{3+}:YAG has been recorded under excitation at 351 nm ($^6H_{15/2}\rightarrow{}^6P_{7/2}$) and emission at 482nm ($^4F_{9/2}\rightarrow{}^6H_{15/2}$). At

lower concentrations the decay curves were well fitted by a single exponential function and at 5 mol%, however, the observed decay curve was bi-exponential. With the increase of Dy^{3+} concentration, the distance between the Dy^{3+} ions decreases; subsequently, the energy transfer between

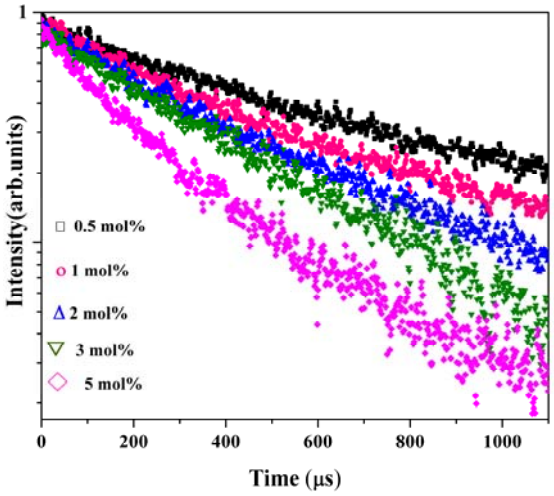

Fig 8. Decay curves of the different concentrations of Dy^{3+}:YAG nanophosphors.

Dy^{3+} ions is more frequent. Therefore the energy transfer process between the Dy^{3+} ions provides an extra decay channel to change the decay curves, resulting in a bi-exponential decay curve. The average life times of these bi-exponential curve was calculated from the formula $(A_1t_1^2+A_2t_2^2)/(A_1t_1+A_2t_2)$. The measured lifetimes are 535, 642, 450, 375 and 280 μs. From the measured lifetimes, it is clear that, when the concentration increases to 1 mol% the lifetime increases to 535 to 642 μs, and when the concentration increases above 1 mol% the life time decreases from 642 to 280 μs. Therefore the lifetimes are well correlated with the emission intensities. The Commission International De I- Eclairage (CIE) chromaticity coordinates for Dy^{3+}:YAG nanophosphors were calculated and represented in Fig. 9. We have observed that the Dy^{3+}: YAG exhibits excellent CIE coordinates of (0.29, 0.35), (0.32, 0.38), (0.30, 0.37), (0.28, 0.35) and (0.26, 0.34) for 0.5, 1, 2, 3 and 5mol%, respectively, which are quite close to that of the national television system Committee (NTSC) illuminant white light point (0.3101, 0.3162), high definition television (HDTV) system illuminant white light point (0.3127, 0.329) and color match illuminant white light point (0.3457, 0.3585). This makes it possible to make a near UV- white LED capable of emitting cool white desired for outdoor illumination applications, temperature sensors and also useful for optical display systems. The above observations hint at the promising application of Dy^{3+}: YAG nanophosphors to produce white-light for near UV-LEDs as well as optical display systems

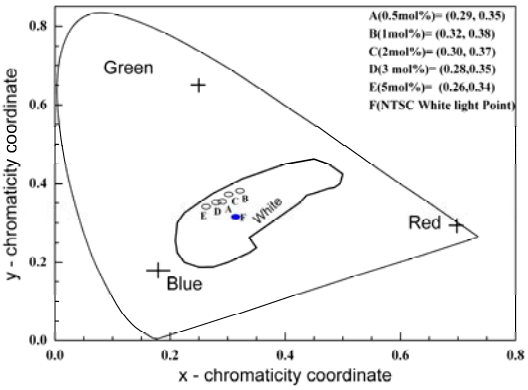

Fig. 9. CIE diagram represented with our obtained chromaticity coordinates

4. Conclusions

We have successfully been synthesized a series of Dy^{3+} ions activated YAG nanophosphors by means of solvothermal process and sintering at various temperatures. The structural and the luminescent properties of Dy^{3+}: YAG nanophosphors have been studied by the measurement of their XRD, SEM, PLE and PL spectra. The emission spectra show two strong bands in blue ($^4F_{9/2}\rightarrow{}^6H_{15/2}$) and yellow ($^4F_{9/2}\rightarrow{}^6H_{13/2}$) regions. Based on the emission spectra, we could calculate the chromaticity coordinates of Dy^{3+}: YAG nanophosphors and which approaches the NTSC, HDTV and color match illuminant white light condition. Such luminescent nanophosphors could be suggested as an ideal optical material for the development of white light emitting optical display systems and lamps.

Acknowledgements

This work was supported by the Korea Research Foundation(KRF) grant funded by the Korea government(MEST) (No. 2009-0076967), and also partially supported by NCRC(National Core Research Center) program through the National Research Foundation of Korea funded by the Ministry of Education, Science and Technology (2010-0001-226).

References

[1] Handbook of luminescence, display materials and devices, edited by H S Nalwa, L S Rohwer (American Scientific Publishers) vol.2(2003)
[2] C. Feldmann, T. Jüsatel, C.R. Ronda, P.J. Schmidt, Adv. Funct. Mater. 13, 511 (2003)
[3] Inorganic phosphors; compositions, preparation and optical properties, edited by Yen W M, Weber M J (CRC Press) vol.20(2004)
[4] Practical applications of phosphors, edited by William M. Yen, Shigeo Shionoya, Hajime Yamamoto (CRC Press) (2006)

[5] S. K.Singh, K. Kumar, S. B. Rai, Appl.Phys. B, **94**, 165 (2009).
[6] O.V. Salata, J. Nanobiotec. **2,** 3 (2004)
[7] L. Wen, X. Sun, Z. Xiu, S. Chen, C. T. Tsai, J. Eur.Ceram. Soc.**24**, 2681 (2004)
[8] A. Ikesue, I. Furusato, K. Kamata, J. Am. Ceram. Soc. **78**, 225 (1995)
[9] K. Keller, T. Mah, A. Parthasarathy, Ceram. Eng. Sci. Proc., **11**, 1122 (1990)
[10] J. B. Willis, M. Dixon, J. Cryst. Growth, **3**/4, 236 (1968)
[11] R. F. Belt, R. C. Puttbach, D. A. Lepore, **13/14**, 268 (1972)
[12] R. Manalert, M. N. Rahaman, J. Mater. Sci. **31**, 3453(1996)
[13] S. M. Sim, K. A. Keller, J. Mater. Sci. **35**, 713 (2000).
[14] J. W. G. A. Vrolijk, J. W. M. M. Willems, R. Metselaar, J. Eur. Ceram. Soc. **6**, 47 (1990)
[15] J. Kuang, Y. Liu, J. Zhang, J. Solid State Chem.**179**, 266 (2006).
[16] B. Liu, L. Kong, C. Shi, J. Lumin. **122-123**, 121 (2007)
[17] D. Jia, Y. Wang, X. Guo, K. Li, Y.K. Zou, W. Jia, J. Electrochem. Soc. **154**(1), J1 (2007)
[18] F. L. Yuan, H. J. Ryu, Mater. Sci. Eng. *B* 107, 14 (2004)
[19] J. Y. Choe, D. Ravichandran, S. M. Blomquist, K. W. Kirchner, E. W. Forsythe, D. C. Morton, J. Lumin. **93**, 119 (2001)
[20] S. K. Shi, J. Y. Wang, Chin. J. Inorg. Chem. **18**, 431 (2002)
[21] G. Zou, H. Li, Y. Zhang, K. Xiong,Y. Qian, Nanotechnol.**17**, S313 (2006)
[22] Y. C. Kang, Y. S. Chung, and S. B. Park, J. Am. Chem. Soc. **82**, 2056 (1999)
[23] M. Veith, S. Mathur, A. Kareiva, M. Jilavi, M. Jimmer, V. Huch, J. Mater. Chem. **9**, 3069(1999)
[24] Y. Zhou, J. Lin, M. Yu, S. Wang, J. Alloys Compd. **375**, 93 (2004)
[25] L.P.Goss, A.A. Smith, M.E.Post, Rev. Sci. Instrum. **60**, 3702(1989)
[26] W-N. Wang, W. Widiyastuti, T. Ogi, I.W. Lenggoro, K. Okuyama, Chem. Mater **19**, 1723(2007)
[27] W.T.Carnall, P.R.Fields, K.Rajnak, J.Chem.Phys. **49**, 4424 (1968)
[28] J. Mulak, M. Mulak, J. Phys. A: Math. Theor. **40**, 2063 (2007)
[29] J. B Gruber, B. Zandi, U.V. Valiev, Sh. A. Rakhimov, J.Appl.Phys. **94**, 1030 (2003)
[30] T. Kano, in Phosphor Handbook (second edition), edited by W.M.Yen, S. Shionoya and H. Yamamoto (CRC Press, 2006), Chap.3. p.205-210
[31] H.Xu, H. Yang, Phys. Stat. Sol. (a). **204**, 1203(2007)
[32] E. Antic-Fidancev, J. Holsa, M. Lastusaari, A. Lupei, Phys. Rev. B. **64**, 195108(2001).

*Corresponding author: bkmoon@pknu.ac.kr